



Electromagnetic interference shielding effectiveness of MgO–Al₂O₃–SiO₂ glass–ceramic system

PREETI KUMARI*, PANKAJ TRIPATHI, OM PARKASH and DEVENDRA KUMAR

Department of Ceramic Engineering, Indian Institute of Technology (Banaras Hindu University),
Varanasi 221 005, India

*Author for correspondence (preetikumari5501@gmail.com)

MS received 24 November 2016; accepted 14 April 2017; published online 7 December 2017

Abstract. MgO–Al₂O₃–SiO₂ (MAS)-based glass–ceramic system was prepared using very-low-cost raw materials, i.e., talc, calcined alumina and calcined china clay with titanium dioxide as a nucleating agent. Glass–ceramics were prepared by a two-step process. In the first step, raw materials were mixed in the required proportion and melted at 1450°C followed by water quench into a glassy frit. In the second step, powdered glass frit was uniaxially dry pressed into pellets followed by sintering at 1200°C for 3 h. X-ray diffraction pattern of the sintered compact shows well-defined peaks of cordierite along with some anorthite and magnesium titanium oxide. The microstructure study of sample shows the presence of crystalline and glassy phases. Permittivity and permeability measurements were performed in the microwave frequency range 12.4–17 GHz. The permittivity value of 5.7–6.0 and the permeability value of ~1 were obtained. The reflection and transmission measurements show that the material possesses a shielding effectiveness in the range 2–10 dB over the frequency range 12.4–17 GHz.

Keywords. Microwave shielding; glass–ceramics; nucleating agent.

1. Introduction

In the present era of advanced technologies, electronics and communications systems operating in the gigahertz (GHz) frequency range are growing at a very fast pace in the consumer market. The electromagnetic (EM) radiations produced by the radio, telephone, microwave transmission, satellite systems, etc. interfere with each other, resulting in electromagnetic interference (EMI). A large number of base stations, continuously multiplying, are becoming sources of high levels of non-ionizing EM radiation. This results in a serious problem of EM pollution. EMI also deteriorates the performance of electronic devices. Therefore, developing new cost-effective materials possessing EM shielding properties is required, so that they can be used for shielding devices sensitive to EM field. Another concern that cannot be ignored is the effect of EM radiation on human health. Even low-frequency band of microwave fields may affect human health. Exposure of EM waves for long duration causes health hazards such as symptoms of anxiety, depression, insomnia, nervousness, headache and languidness [1,2]. Many research workers have studied various material like polyvinylidene fluoride (PVDF)–barium titanate composites, multi-walled carbon nanotube–polymer nanocomposite, composites of butyl-rubber and single-walled carbon nanotubes, hybrids based on PVDF and Cu nanoparticles, graphene oxide-deposited carbon fibre composites, cement composites using carbonaceous nano/micro-inerts, etc. for EM shielding applications [3–7]. These materials

can be utilized in protecting various electronic equipment and can make the equipment more efficient and precise. However, the carbon-based EMI shielding materials lack mechanical flexibility. Metal-based EMI shielding materials have the disadvantage of heavy weight and corrosion. Polymer-based EMI shielding material like poly-aniline lacks flexibility and mechanical strength [1]. Therefore, environmentally stable and commercially viable shielding materials are required in large quantities for buildings or anechoic chambers. For meeting different aspects of the EM shielding requirements in widespread applications, where large quantities of materials are required, cost becomes an important factor. Glass–ceramics from low-cost raw materials and simple processing techniques may hold great potential for such applications.

Glass–ceramics are partially crystalline materials with one or more crystalline phases embedded in an amorphous glassy matrix [8–10]. It has been shown that glass–ceramics exhibit higher hardness and scratch resistance than those of parental glasses or even conventional ceramics [11]. Magnesium alumino-silicate (MAS) glasses and glass–ceramics with major alpha cordierite phase have attracted attention from industrialists and researchers for their wide applications [12–14]. They are known for their good mechanical properties, e.g., high surface hardness, strength, fracture toughness and abrasion resistance; good thermal properties like thermal shock resistance and thermal stability; chemical stability and marble-like appearances [14–18]. These glass–ceramics can

Table 1. Chemical analysis of starting raw materials.

Raw materials	SiO ₂	Al ₂ O ₃	Fe ₂ O ₃	TiO ₂	CaO	MgO	K ₂ O	Na ₂ O
Calcined china clay	52.52	41.13	1.3	2.27	0.83	0.97	0.7	0.28
Talc powder	61.1	2	0.68	0.21	2.63	32.24	0.62	0.52
Calcined alumina	—	99.57	0.01	—	0.04	—	—	0.38
TiO ₂	0.1	1.52	0.1	97.81	0.12	0.1	0.15	0.1

also be produced in large quantities by utilizing industrial waste like fly ash from thermal power plants and iron ore tailings from steel industry [19–22], which can be used as glazes on vitrified ceramic tiles used in buildings [8, 18, 23, 24]. Many researchers have studied the phase transformation, crystallization behaviour and properties of MAS-based glass–ceramic system by changing various processing parameters [25–27].

To the best of our knowledge, there are no glasses or glass–ceramic material standalones for the EMI shielding application, although there are some EMI shielding glasses made from float glass with a conductive coating on one side. This glass gives EMI shielding behaviour along with high light transmission, which makes it suitable for electronic displays [28]. The light transmittance and the RF shielding effectiveness of a gold film on a glass substrate have also been investigated four decades ago [29].

The objective of the present work is to determine the EMI shielding effectiveness of MAS glass–ceramic system doped with TiO₂. These glass–ceramics are prepared from commercially available cheap talc, calcined alumina and calcined china clay as raw materials. The prepared MAS glass–ceramics show good EMI shielding effectiveness and can be used as glaze for vitrified ceramic tile in anechoic chambers or buildings.

2. Experimental

MgO–Al₂O₃–SiO₂ glass–ceramic was prepared using talc, calcined alumina, calcined china clay and titanium dioxide. The chemical composition of starting raw materials is presented in table 1. The batch was formulated by mixing talc, calcined alumina, calcined china clay and titanium dioxide in proportions by weight percent of 45, 15, 30 and 10, respectively. Batch composition and molar ratio are given in table 2. TiO₂ was used as a nucleating agent. Ball milling of batch composition was done for 24 h for proper mixing and grinding. After homogeneous mixing, the batch was melted in an alumina crucible at 1450°C in an electric furnace. Quenching was done by pouring the melt into water. The glass frit obtained was crushed, finely ground to 300 mesh, sieved and dried. DTA of sample was performed using LABSYSTM Setaram Instrumentation in the temperature range 50–1200°C, at a heating rate of 10°C min⁻¹ in argon atmosphere. Cylindrical test pellets having 15 mm diameter

Table 2. Composition of initial powder calculated based on chemical analysis of starting raw materials.

Raw materials	Batch composition (wt%)
Calcined china clay	30
Talc powder	45
Calcined alumina	15
TiO ₂	10
MgO–Al ₂ O ₃ –SiO ₂ –TiO ₂ (molar ratio) (2.8:2.1:5.5:1)	

were compacted under 100 MPa pressure in a hydraulic press. All green pellets were sintered at 1200°C for 3 h. Powder X-ray diffraction (XRD) was carried out using a Rigaku High Resolution Powder X-ray Diffractometer employing Cu K α ₁ radiation (1.5406 Å) and Ni filter to identify the different crystalline phases in glass–ceramics. Microstructural study of the chemically etched sample (10% HCl + 5% HF solution for 30 s) was carried out using a scanning electron microscope. The energy-dispersive spectrum (EDS) was used for elemental analysis. S-parameter measurements were performed by the waveguide method (Nicholson–Weir–Ross technique) using a network analyser E5071C (Keysight Tech.) to obtain permittivity, permeability, shielding effectiveness, skin depth and conductivity.

3. Results and discussion

The DTA graph (figure 1) shows the glass transition temperature and peaks of primary and secondary crystallization for the aforementioned MAS composition. The base line shift at 786°C corresponds to glass transition temperature. Exothermic peaks at temperatures 891, 978 and 1053°C correspond to crystallization of different phases. Figure 2 shows XRD patterns of the MAS glass–ceramic sample sintered at 1200°C. It can be observed that MAS glass–ceramic samples have the main crystalline phase of cordierite (PDF 84-1219). Small amounts of anorthite (PDF 41-1486) and MgO · 2TiO₂ (PDF 20-0694) are also present as secondary phases.

In figure 3, the SEM micrographs of MAS glass–ceramic at different magnifications are shown. The phases of cordierite, anorthite and magnesium titanium oxide are present in the microstructure, which is confirmed by the XRD analysis also.

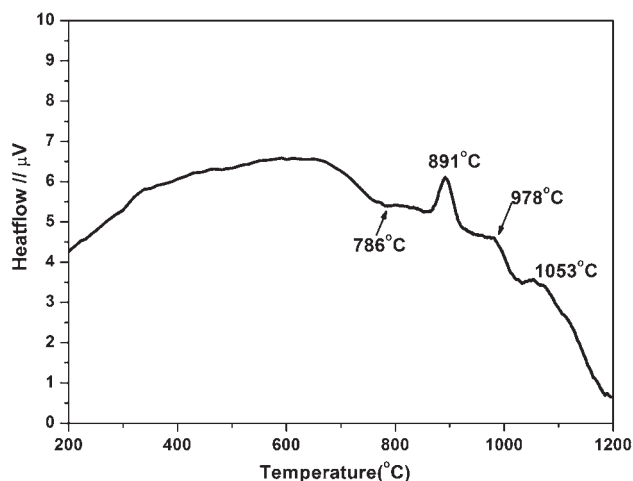


Figure 1. DTA curve of powder MAS glass frit.

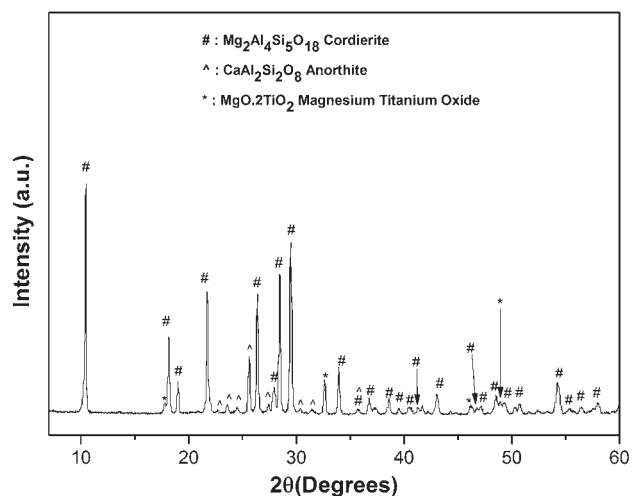


Figure 2. Powder XRD pattern of MAS glass–ceramic sample.

The major part of the microstructure consists of the hexagonal prismatic morphology, which represents the cordierite phase formation. White acicular crystals indicate the presence of magnesium titanium oxide. EDS of MAS glass–ceramics at the three sites marked as (a), (b) and (c) is shown in figure 4. The EDS spectrum of site (a) indicates the presence of cordierite and anorthite. At site (b), the peak of Mg and Ti is very much significant in the spectrum, which indicates the presence of magnesium titanium oxide phase. Site (c) represents complete microstructural area of the sample for the EDS analysis. In the MgO–Al₂O₃–SiO₂ ternary system, the primary cordierite phase is formed at lower temperatures and develops to become hexagonal prismatic structures at higher temperatures. It is also observed during the development of hexagonal prisms that the inner central area is not fully formed and gets occupied by the secondary phases like anorthite or glass particles rich in CaO [24]. The small white particles present over the large hexagonal cordierite grains in figure 3

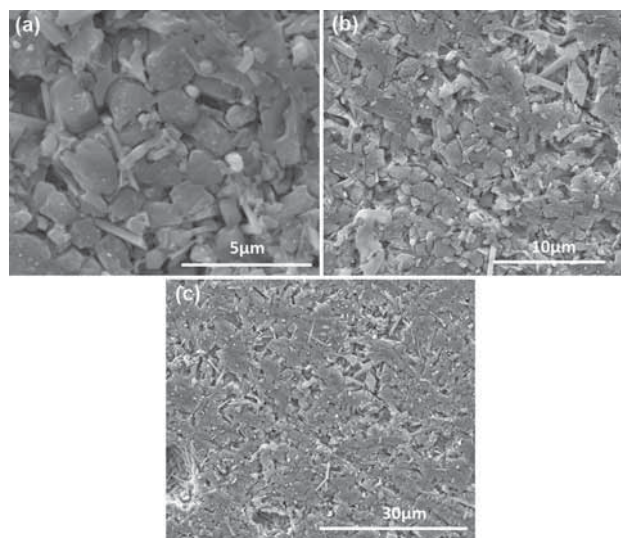


Figure 3. SEM micrographs of MAS glass–ceramic sample at different magnifications: (a) 25000×, (b) 10000× and (c) 5000×.

are probably the anorthite crystals, also confirmed by EDS. SEM image (figure 3) of MAS glass–ceramic shows contrast change between grains (brighter) and glassy phase (darker). Several grains are embedded half inside the glass with others located below the surface. Due to incomplete etching, residual glass with irregular shape may stick to grains or cover partially several adjacent grains possibly.

The experimental bulk density of the sintered MAS glass–ceramic samples is found to be $\sim 2.57 \text{ g cm}^{-3}$. The permittivity and permeability values of the MAS glass–ceramic sample measured in the frequency range 12.4–17 GHz are presented in figure 5. In the GHz frequency range the atomic polarization and vibronic modes are the main phenomenon that contributes to the permittivity values. The vector network analyser utilizes the Nicholson–Weir–Ross technique [30] to evaluate permittivity and permeability using measured S -parameters. It is observed that the average permittivity value is around six and the average permeability μ values are nearly one in the frequency range 12.4–17 GHz. The total EMI shielding effectiveness (SE_T) is the sum of absorption and reflection shielding effectiveness:

$$SE_T = SE_A + SE_R. \quad (1)$$

It includes the power loss during transmission by the absorption and reflection mechanism. The S_{11} and S_{21} parameters are measured in the reflection and transmission mode. The power loss by absorption during transmission is given by

$$SE_A = -10 \log[S_{21}^2 / (1 - S_{11}^2)] \quad (2)$$

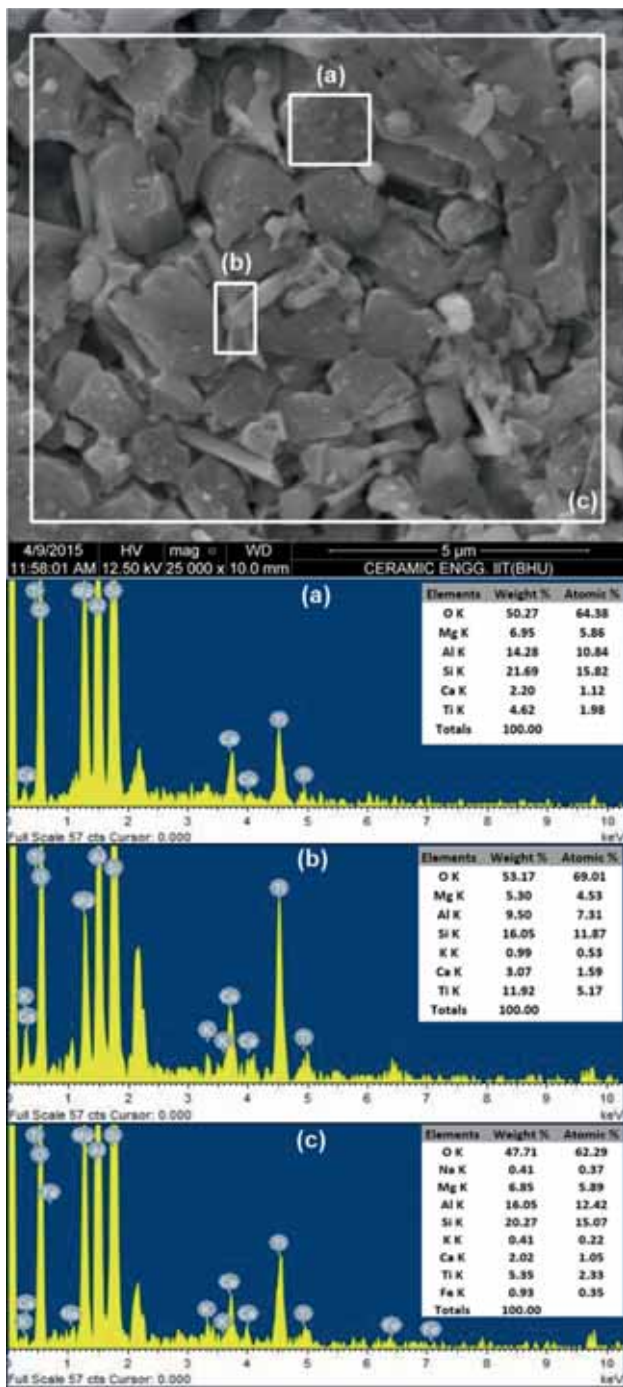


Figure 4. EDS analysis of MAS glass–ceramic sample.

and called as absorption shielding effectiveness (SE_A). The power loss by reflection during transmission is given by

$$SE_R = -10\log[1 - S_{11}^2] \tag{3}$$

and called as reflection shielding effectiveness (SE_R) [31,32]. The variation of shielding effectiveness of MAS glass–ceramic sample as a function of frequency is shown in figure 6.

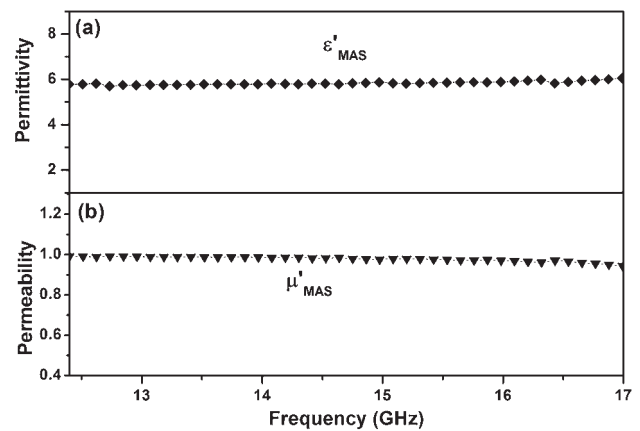


Figure 5. Variation of (a) permittivity and (b) permeability of MAS glass–ceramic sample with frequency.

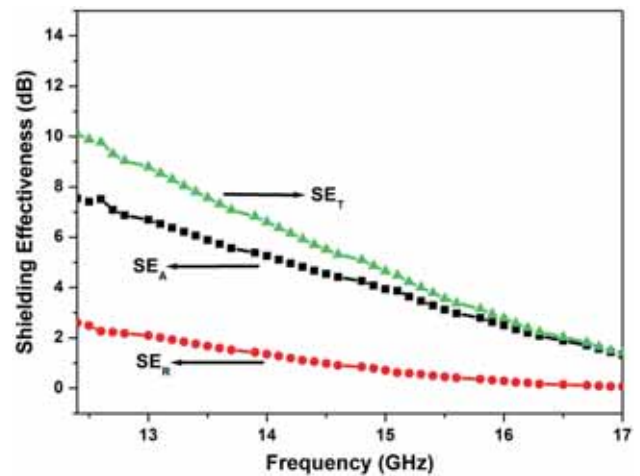


Figure 6. Variation of shielding effectiveness of MAS glass–ceramic sample with frequency.

The shielding effectiveness is found to be good, i.e., 6–10 at lower frequencies (12.4–15 GHz), while it decreases up to 2 dB in the higher frequency range (15–17 GHz).

Skin depth is also a very important parameter for considering the material for microwave shielding application. At high frequencies, the EM radiation penetrates only the near-surface area of a conductor. The skin depth can be defined as the distance up to which EM wave gets attenuated by $1/e$ or 0.37 [33].

The skin depth δ is a function of conductivity σ , absolute permeability μ and frequency f and given as

$$\delta = (\pi f \mu \sigma)^{-1/2}. \tag{4}$$

The variation of skin depth of MAS glass–ceramic sample is shown in figure 7a, which shows that less thickness of material is required as frequency increases towards 17 GHz. The ac conductivity of MAS glass–ceramics is calculated. From figure 7b, it is observed that the ac conductivity

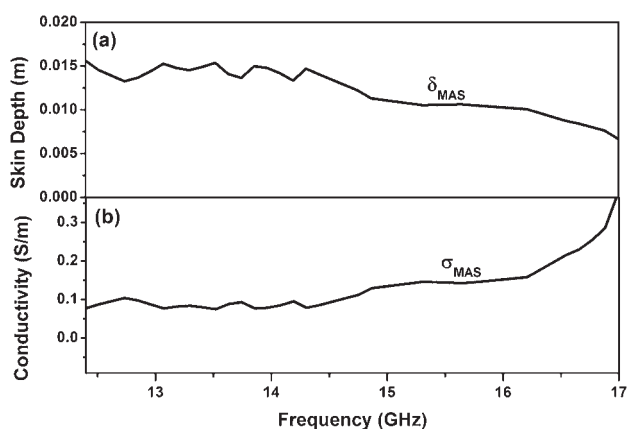


Figure 7. Variation of (a) skin depth and (b) conductivity of MAS glass–ceramic sample in the frequency range 12.4–17 GHz.

value rises with frequency and is found to be in the range 0.084–0.415 S m⁻¹.

4. Conclusions

A MAS glass–ceramic was prepared by the conventional solid-state method using low-cost raw materials. DTA shows three exothermic crystallization peaks at 891, 978 and 1053°C. XRD pattern of sintered glass–ceramic sample shows well-formed peaks of cordierite as the major phase along with the co-existence of anorthite and magnesium titanium oxide as secondary phases. The microstructure and EDS also confirm the existence of cordierite, anorthite and magnesium titanium oxide phases. Permittivity values 5.7–6.0 and permeability values ~ 1 are found in the frequency range 12.4–17 GHz. The glass–ceramic material shows good shielding effectiveness in the range ~ 2 –10 dB with skin depth 0.006–0.015 m. The prepared MAS glass–ceramics with EMI shielding effectiveness can be used as glazes on vitrified ceramic tiles for shielding buildings or anechoic chambers.

References

- [1] Geetha S, Kumar K K S, Rao C R K, Vijayan M and Trive D C 2009 *J. Appl. Polym. Sci.* **112** 2073
- [2] Kumar M, Singh S P and Chaturvedi C M 2016 *Exp. Neurobiol.* **25** 318
- [3] Chen J, Zhao D, Ge H and Wang J 2015 *Constr. Build. Mater.* **84** 66
- [4] Khushnood R A, Ahmad S, Savi P, Tulliani J M, Giorelli M and Ferro G A 2015 *Constr. Build. Mater.* **85** 208
- [5] Yim Y J and Park S J 2015 *J. Ind. Eng. Chem.* **21** 155
- [6] Verma P, Saini P and Choudhary V 2015 *Mater. Des.* **88** 269
- [7] Arranz-Andres J, Perez E and Cerrada M L 2012 *Eur. Polym. J.* **48** 1160
- [8] Casasola R, Rincon J M and Romero M 2012 *J. Mater. Sci.* **47** 553
- [9] James P 1995 *J. Non-Cryst. Solids* **181** 1
- [10] Holand W and Beall G H 2012 *Glass ceramic technology* (Hoboken, New Jersey: John Wiley & Sons)
- [11] Stookey S 1959 *Ind. Eng. Chem.* **51** 805
- [12] Ohsato H, Kim J S, Cheon C I and Kagomiya I 2015 *Ceram. Int.* **41** S588
- [13] Sohn S B, Choi S Y and Lee Y K 2000 *J. Mater. Sci.* **35** 4815
- [14] Seidel S, Patzig C, Wisniewski W, Gawronski A, Hu Y, Hoche T *et al* 2016 *Sci. Rep.* **6** 34965
- [15] Yao R, Liao S, Dai C, Yang Y and Zheng F 2014 *Ceram. Int.* **40** 8667
- [16] Wange P, Hoche T, Russel C and Schnapp J D 2002 *J. Non-Cryst. Solids* **298** 137
- [17] Gawronski and Russel C 2013 *J. Mater. Sci.* **48** 3461
- [18] Casasola R, Rincon J M and Romero M 2012 *J. Mater. Sci.* **47** 553
- [19] Yao R, Liao S Y, Dai C L, Liu Y C, Chen X Y and Zheng F 2015 *J. Magn. Magn. Mater.* **378** 367
- [20] Sampathkumar N N, Umarji A M and Chandrasekhar B K 1995 *Mater. Res. Bull.* **30** 1107
- [21] Erol M, Kucukbayrak S and Ersoy-Mericboyu A 2008 *J. Hazardous Mater.* **153** 418
- [22] Kim Jae M and Kim H S 2004 *J. Eur. Ceram. Soc.* **24** 2825
- [23] Torres F J and Alarcon J 2005 *Ceram. Inter.* **31** 683
- [24] Torres F J and Alarcon J 2003 *J. Eur. Ceram. Soc.* **23** 817
- [25] Guo X, Cai X, Song J, Yang G and Yang H 2014 *J. Non-Cryst. Solids* **405** 63
- [26] Rezvani M, Eftekhari-Yekta B, Solati-Hashjin M and Marghussian V K 2005 *Ceram. Int.* **31** 75
- [27] Banjuraizah J, Mohamad H and Ahmad Z 2010 *Int. J. Appl. Ceram. Technol.* **8** 637
- [28] www.hollandshielding.com
- [29] Liao S Y 1975 *IEEE Trans. Electromagn. Compat.* **EmC-17** 211
- [30] Tripathi P, Sahu B, Singh S P, Parkash O and Kumar D 2015 *Ceram. Int.* **41** 2908
- [31] Joseph Nina, Janardhanan C and Sebastian M T 2014 *Compos. Sci. Technol.* **101** 139
- [32] Joseph Nina, Singh S K, Sirugudu R K, Murthy V R K, Ananthakumara S and Sebastian M T 2013 *Mater. Res. Bull.* **48** 1681
- [33] Farukh M, Singh A P and Dhawan S K 2015 *Compos. Sci. Technol.* **114** 94